

Active Learning Guided Federated Online Adaptation: Applications in Medical Image Segmentation

Md Shazid Islam*, Sayak Nag, Arindam Dutta,
 Miraj Ahmed, Fahim Faisal Niloy, Amit K. Roy-Chowdhury
 Video Computing Group
 Department of Electrical and Computer Engineering,
 University of California Riverside,
 Riverside, California, USA

Abstract

*Data privacy, storage, and distribution shifts are major bottlenecks in medical image analysis. Data cannot be shared across patients, physicians, and facilities due to privacy concerns, usually requiring each patient's data to be analyzed in a discreet setting at a near real-time pace. However, one would like to take advantage of the accumulated knowledge across healthcare facilities as the computational systems analyze data of more and more patients while incorporating feedback provided by physicians to improve accuracy. Motivated by these, we propose a method for medical image segmentation that adapts to each incoming data batch (online adaptation), incorporates physician feedback through active learning, and assimilates knowledge across facilities in a federated setup. Combining an online adaptation scheme at test time with an efficient sampling strategy with budgeted annotation helps bridge the gap between the source and the incoming stream of target domain data. A federated setup allows collaborative aggregation of knowledge across distinct distributed models without needing to share the data across different models. This facilitates the improvement of performance over time by accumulating knowledge across users. Towards achieving these goals, we propose a computationally amicable, privacy-preserving image segmentation technique **DrFRODA** that uses federated learning to adapt the model in an online manner with feedback from doctors in the loop. Our experiments on publicly available datasets show that the proposed distributed active learning-based online adaptation method outperforms unsupervised online adaptation methods and shows competitive results with offline active learning-based adaptation methods.*

1. Introduction

Image segmentation is a fundamental task in medical image analysis as accurate medical image segmentation facilitates treatment [29], rehabilitation [19], and long-time disease monitoring [21] by analyzing the precise shape of internal organs and detecting abnormalities. In recent years, deep learning based medical image segmentation [2,28] has shown impressive performance gains and pragmatic use for diagnosis and treatment [1]. However, these models require extensive fully-annotated training data to handle diverse datasets with variations in imaging modalities, quality, and demographics [9]. This presents two major bottlenecks: firstly, centralized assembly of medical images from numerous patients is not a viable option due to a breach of doctor-patient confidentiality [13,27], alongside considerable logistical challenges associated with data storage and secondly, the acquisition of pixel-level annotations for large-scale medical imaging is time-consuming and expensive. To address these concerns, we propose to address the problem of medical image segmentation in a federated learning setup [32]. Additionally, we consider a practical setting where medical data arrives to the radiologist in a streaming fashion [34] and the radiologist has the scope of annotating an extremely limited number of pixels [36].

In order to address the first bottleneck of privacy and storage of medical images, we propose to use a federated learning setup. Federated learning (FL) facilitates distributed training of multiple models on numerous datasets without sharing the data among the local models or the central server. The central server maintains a global model, the parameters of which are updated as an aggregate of those of the local models [38]. Since the local models are deployed by individual healthcare centers, they will be exposed to variations in patient data across these centers. Due to the federated learning setup, the global model will be inevi-

*Corresponding author. Email: misla048@ucr.edu

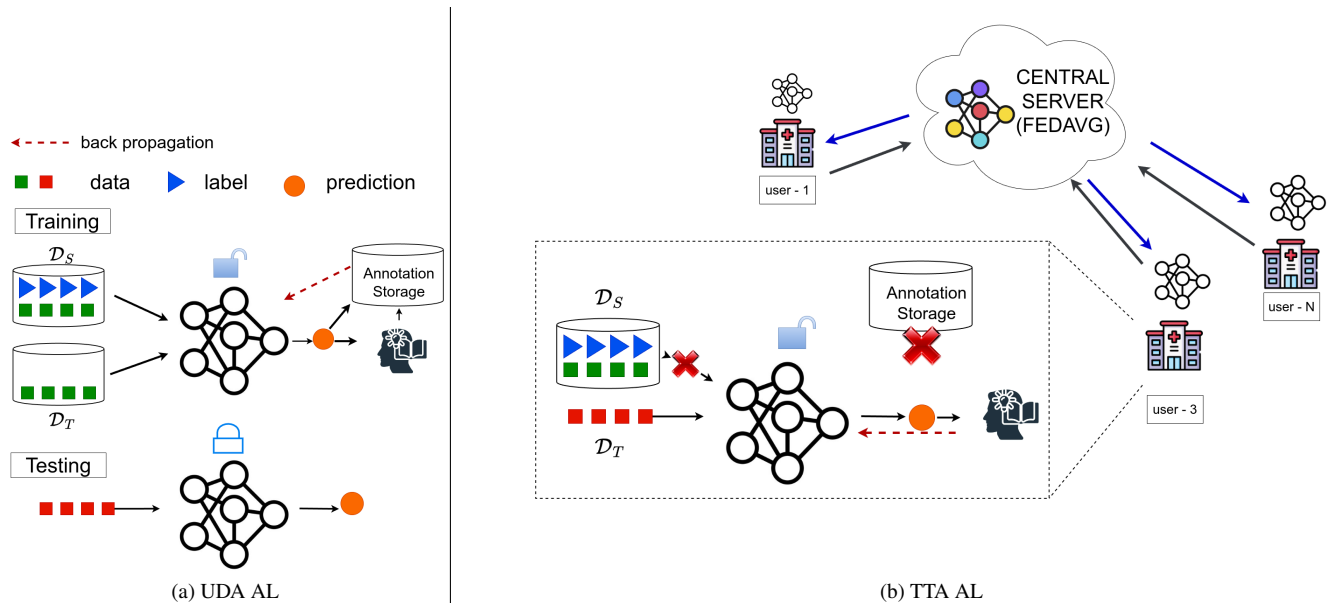


Figure 1. Figure 1a illustrates the offline UDA with AL setup, where both source and target domain data must be aggregated into a central location for training. Figure 1b illustrates our federated TTA with active learning setup, where we do not allow any access to source data or any kind of data storage.

dently exposed to these variations via the parameters of the local models. However, the federated learner must be able to adapt to the diverse forms of data distribution that can occur in medical images. An example of such variations is the distribution shift in MRI images of the same person captured by machines supplied by two different vendors [17].

In order to address the second bottleneck of the necessity of distribution exhaustive heavily annotated pixel-level training data, unsupervised domain adaptation (UDA) has been proposed as an effective approach in the literature [4, 18, 33]. The core idea of UDA is to use the available labeled data from a source domain along with unlabeled data from the target domain to perform self-training of a model in order to minimize the distribution shift and hence, adapt it to the target domain [36]. However, most existing UDA methods rely on two major assumptions: access to the labeled source data for empirical risk minimization and, availability of the entire target domain training data. For both cases, data storage and privacy are major concerns as a large-scale centralized database has to aggregate patient medical data from different sources to enable such offline adaptation [13, 27]. In practical health-care settings, a physician has to deal with a continuous flow of patients with no knowledge about the future patient, making existing offline UDA approaches [4, 18, 33] ineffective for real-time deployment. This motivates us to develop a real-time online adaption algorithm for the federated learning setup. This form of online adaptation that does not require the source data and uses only an incoming batch of target

domain test data to optimally adapt the model to this target domain is colloquially referred to as Test Time Adaptation (TTA) [6, 8, 11]. TTA enables model adaptation through a single pass of an online test batch, bypassing the need for multiple backward passes, which would require the storing of the batched data, as is the case in standard UDA [36]. The integration of TTA with a federated learning setup is relatively unexplored in literature. Due to the importance of distributed online learning for medical image segmentation, we propose an effective integration of TTA with federated learning. Figure 1 shows the difference between our federated TTA setup and standard UDA-based segmentation setup.

Although TTA is a more effective option compared to standard UDA for on-the-fly adaptation, in a federated learning setup, the local models adapted using TTA might exhibit sub-optimal adaptation performance on encountering data from a target domain with extremely varied distribution compared to the source distribution on which the model was originally trained on. Such varied distributions of target data might even lead to catastrophic forgetting of the source knowledge resulting in the model learning trivial solutions [35]. In such situations, limited annotation feedback from the radiologists will aid the local models toward optimal adaptation and consequently boost the overall performance of the global model itself.

The distributed setup of federated learning will encompass multiple annotators at the local level as opposed to having a single annotator as in the non-distributed setup.

This also enables collaborative training among health facilities without explicitly sharing their individual and diverse set of private patient data, while also mitigating their individual local model’s ineffectiveness in handling previously unseen variations in patient data. Motivated by these findings we propose an effective active learning guided federated TTA framework called **DrFRODA: Doctors-in-the-loop Federated Online Domain Adaptation**. **DrFRODA**. To the best of our knowledge, *this is the first paper to propose active learning guided TTA for a federated learning process*.

DrFRODA incorporates an innovative subset selection strategy involving selective image pruning that minimizes the annotation burden of the radiologist, enabling the selection of the minimal but most informative subset of pixels from the most relevant images from each batch of target domain test images. Our framework needs a model pre-trained on the source domain to begin the adaptation process which is distributed across numerous local users (doctors/healthcare centers). Every local model encounters a distinct online batch of target domain test images and produces pixel-wise pseudo labels. Using selective image pruning most informative images are first selected from the test batch and their pixel-wise pseudo labels are used for uncertainty-guided budgeted sampling of pixels to be annotated by the doctor. Since a doctor can access only his patient’s data for active learning, it prevents privacy breaches. The active feedback from the doctor is used to update the local models via supervised empirical risk minimization on the active pixels. As per the federated learning setup, only the parameters (weights and biases) of the local models are transferred to the central server, which are aggregated by FedAvg [23] to update the global model, thereby mitigating concerns of privacy, storage and distribution shifts in medical images. The major contributions of this work are summarized as follows:

- We propose **DrFRODA**, a novel federated TTA framework with doctors-in-the-loop active learning for storage-efficient and privacy-preserving medical image segmentation. **DrFRODA** is the first setup to explore both federated TTA and the integration of active learning to the same.
- We propose a novel image pruning strategy to significantly reduce the annotation burden on each local user.
- We perform extensive experimentation on publicly available medical image datasets and show that with as little as 1% annotations acquired as active feedback, **DrFRODA** not only outperforms existing TTA approaches by a considerable margin but also reaches near offline UDA performance.

2. Related Works

Test Time Adaptation. Unsupervised Domain Adaptation (UDA) is generally an offline adaptation technique which may or may not require the source data for adaptation. However, a large volume of unlabelled data from target domain is necessary to perform the adaptation. This particular configuration is not suitable for situations where a continuous flow of data is present and adaptation needs to be done on the fly. Test time adaptation (TTA) addresses this issue by adapting the model weights according to the characteristics of the current test batch in the target domain. The method TENT [34] adapts the weights of pre-trained source model to target domain by updating only the batch-norm parameters using entropy minimization. EATA [25] proposed a modification of TENT by employing a reliable and non-redundant sample selection method for entropy minimization. CoTTA [34] employed a teacher-student model where all the weights of the student model are updated using consistency loss. Then the teacher model is updated using the exponential moving average method. However, adaptation in TTA methods suffers from catastrophic forgetting which means gradually drifting away from source knowledge. In order to tackle this issue some techniques such as stochastic restoration [35] and fisher regularization [16] have been employed.

Federated Learning. Federated Learning is a decentralized collaborative paradigm for learning with multiple clients where data privacy is preserved for each client. FedAvg [23] is one of the most popular frameworks for federated learning which updates the server model using a weighted average of local models from all clients. The weights of FedAvg are set in proportion to the available data of each client. However, this weighting method is not applicable when the clients have no idea about the volume of future data. Kim *et al.* [14] integrated active learning to federated learning to solve the class imbalance issue. FedSeg [24] proposed a modified cross-entropy loss to address the non IID distribution of foreground and background among the clients.

Active Domain Adaptation. Active learning (AL) is an efficient approach that can reduce the annotation cost while enhancing the performance of deep learning models. In order to maximize the performance of the deep learning model with a budget annotation an effective sampling function is needed. A common strategy is selecting the most uncertain samples. The uncertainty can be measured in terms of entropy [10], Maximum Normalized Log-Probability [30], and Bayesian uncertainty measurement [5]. Annotation for segmentation tasks, especially for images from a new domain, are more expensive and time-consuming than classification task because segmentation involves dense prediction. To address this researchers have incorporated active learning with the standard UDA setup, colloquially referred to as Active Domain Adaptation (ADA). RPU [36] designed

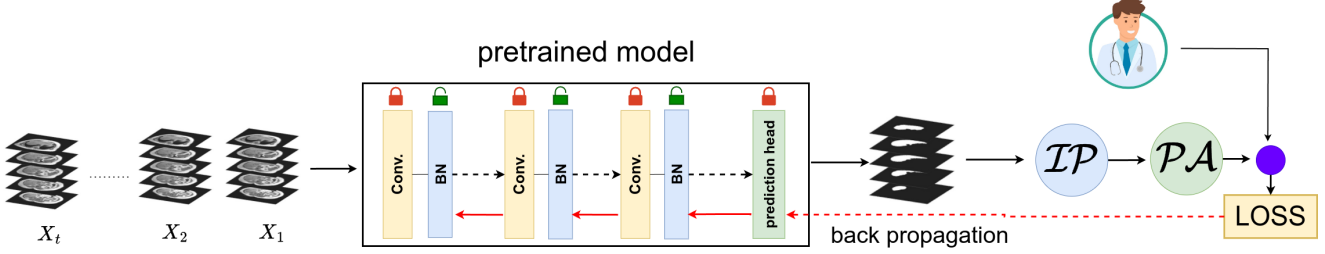


Figure 2. **Local Model Update.** Each local model encounters a continuous stream of batched target domain test images. The model first *infers* the semantic labels of the current batch and obtains the pixel-wise pseudo-labels. Following this, the local active learning block first uses \mathcal{IP} to prune the test batch (Sec 3.2.1) and obtain the subset of the most informative images in the batch. Next, the pseudo labels of the selected images are passed to the pixel acquisition block \mathcal{PA} (Sec 3.2.2) which selects $b\%$ of most uncertain pixels in these images for annotation acquisition from the local user/doctor. Following the acquisition, the BN layers of this model are updated by supervised minimization of cross-entropy loss on the newly annotated pixels.

a sampling strategy based on the uncertainty and regional purity for both pixel and area annotation for the segmentation task. Another methods EADA [37] and LabOR [31] proposed a domain adaptive active learning strategy where samples are selected based on free energy measurement. However, all of these existing strategies are defined for the offline UDA setup and none of the methods show how to acquire annotations from multiple humans across distributed devices i.e. federated learning. Our proposed approach addresses this gap in the literature by showing an effective method for integrating AL in a federated TTA setup.

3. Methodology

3.1. Motivation and Overview

We design an active learning-guided TTA framework for the federated learning setup with application to medical image segmentation. Therefore, we have a set of N distributed to local users and a central server with a global model f_ϕ . f_ϕ is initialized with the parameters of a segmentation model f_ψ trained on a set of labeled source data $\mathcal{S} = \{(X_S^i, Y_S^i)\}_{i=1}^{M_s} \sim \mathcal{D}_s$ to segment total C number of classes, where \mathcal{D}_s is the source domain data distribution.

As shown in Figure 2, following the TTA setup [34] the inference and adaptation process is continuous in nature whereby each user encounters a continuous stream of mini-batches $\mathbf{X}_1^n \rightarrow \mathbf{X}_2^n \rightarrow \dots \rightarrow \mathbf{X}_t^n \rightarrow \dots$ at different steps. Each mini-batch, $\mathbf{X}_t^n = \{X_{\mathcal{T}}^j\}_{j=1}^{B_t}$ where each $X_{\mathcal{T}}^j \in \mathcal{T}$ with \mathcal{T} being the target domain test set sampled from a different data distribution $\mathcal{D}_{\mathcal{T}}$. To prevent any privacy breaches, for any two users (n, m) , at a given time step t , $\mathbf{X}_t^m \cap \mathbf{X}_t^n = \emptyset$. This further ensures data privacy as each user can be considered a doctor using their local models via an edge device, and the mini-batches are medical images of

their respective patients.

The entire TTA process follows an infer, acquire, and update policy. At $t = 1$, a copy of f_ϕ is provided to each local user, henceforth referred to as f_θ^n . Each user first performs inference on the current mini-batch and then, based on our sampling strategy, highlights images and pixels that need to be annotated via active feedback from the user. After acquiring the annotations, they are used for updating the local models via supervised empirical risk minimization. Following the local update, the parameters of each f_θ^n are then transferred to the central server, where f_ϕ is updated through weighted FedAvg [23]. The updated f_ϕ is then redistributed to all the local users for inference on their respective next mini-batch. This form of active feedback guided TTA enables the global model to improve progressively with each incoming stream of test data.

In the subsequent sections, we first describe our local active learning process, followed by the domain adaption and weighted FedAvg techniques.

3.2. Local Active Learning

First each local model f_θ^n is used to conduct inference on a mini-batch \mathbf{X}_t^n and obtain its pixel-wise classification scores $\mathbf{P}_t^n = \{\mathbf{P}_j\}_{j=1}^{B_t}$. In a standard TTA [34, 35] setup, the classification scores will be directly used for minimizing a pseudo-label based loss for self-training. As discussed earlier, self-training with incorrect pseudo-labels will lead to catastrophic forgetting the source knowledge. To alleviate this, we propose a pixel level annotation acquisition strategy from the local radiologist. However, in a test batch, all the images do not exhibit the same amount of domain shift. We hypothesize that the annotations from active learner can be efficiently utilized if the budgeted annotation is spent on the images with larger domain shifts instead of

annotating all the images of the test batch. Thus, pruning the mini-batch to the most informative images alleviates the annotation burden on the local radiologist, which elaborate upon this section.

3.2.1 Selective Image Pruning

To select the images with larger domain shifts, we leverage the batch-normalization layer (BN) statistics of incoming test batches. The statistics of \mathcal{D}_S are stored in the BN layer of the f_ψ in terms of running mean and running variance. In order to determine the domain shift, we compare the feature statistics for each $X_{\mathcal{T}}^j \in \mathbf{X}_t^n$ with the source statistics. With a domain shift, an abrupt change in feature statistics can be visible in terms of KL divergence [7]. Therefore, for each $X_{\mathcal{T}}^j$ in the mini-batch we first augment it to obtain $\tilde{X}_{\mathcal{T}}^j$. Assuming the per-channel BN layers to exhibit a Gaussian distribution the divergence between the statistics of f_ψ (approximated as $\mathcal{N}(\mu_{l_{c'}}^S, (\sigma_{l_{c'}}^S)^2)$ and the BN statistics of $\tilde{X}_{\mathcal{T}}^j$ (approximated as $\mathcal{N}(\mu_{l_{c'}}^{\mathcal{T}_j}, (\sigma_{l_{c'}}^{\mathcal{T}_j})^2)$ is defined as,

$$\begin{aligned} D(S, \tilde{X}_{\mathcal{T}}^j) &= \sum_l \sum_{c'} \text{KL} \left[\mathcal{N}(\mu_{l_{c'}}^S, (\sigma_{l_{c'}}^S)^2), \mathcal{N}(\mu_{l_{c'}}^{\mathcal{T}_j}, (\sigma_{l_{c'}}^{\mathcal{T}_j})^2) \right] \\ &= \sum_l \sum_{c'} \log \left(\frac{\sigma_{l_{c'}}^{\mathcal{T}_j}}{\sigma_{l_{c'}}^S} \right) + \frac{(\sigma_{l_{c'}}^S)^2 + (\mu_{l_{c'}}^S - \mu_{l_{c'}}^{\mathcal{T}_j})^2}{2(\sigma_{l_{c'}}^{\mathcal{T}_j})^2} - \frac{1}{2}. \end{aligned} \quad (1)$$

The higher the value of $D(S, \tilde{X}_{\mathcal{T}}^j)$ the greater the domain shift. Therefore, we select $K\%$ images from each \mathbf{X}_t^n with the highest values of $D(S, \tilde{X}_{\mathcal{T}}^j)$ and remove the remaining resulting in a pruned batch, $\tilde{\mathbf{X}}_t^n$, with batch size $\tilde{\mathcal{B}}_t < \mathcal{B}_t$.

3.2.2 Pixel Sampling

After obtaining the pruned test batch $\tilde{\mathbf{X}}_t^n$, another sample $b\%$ pixels from each of its images for annotating by the local user. Here b is the active learning budget. For the sampling strategy we incorporate the acquisition function proposed in [36].

First, pixel-wise prediction uncertainty is computed as its predictive entropy as shown below,

$$\mathcal{H}(x, y) = - \sum_c \mathbf{P}(x, y, c) \log \mathbf{P}(x, y, c) \quad (2)$$

where \mathbf{P} is the normalized output (using softmax) of the network prediction, (x, y) is the pixel coordinate, and c is its predicted pseudo label. Next Regional Impurity which indicates whether there is a mixture of different instances in a square area is computed. Following [36] a square of size $(2k+1 \times 2k+1)$ is selected the pixel (x, y) , and its regional impurity is computed as follows,

Algorithm 1 DrFRODA

The N users are indexed by n . Image Selection factor $K\%$, Active learning budget for pixel sampling is $b\%$

Require: Source pre-trained model f_ψ ,

- 1: Initialize parameters of global model f_ϕ and local models $\{f_\theta^n\}_{n=1}^N$ same as the pretrained source model f_ψ
 - 2: calculate $\left\{ (\mu_{l_{c'}}^S, (\sigma_{l_{c'}}^S)^2) \right\}$ which is the BN statistics of f_ψ .
 - 3: **for** each round $t = 1, 2, \dots$ **do**
 - 4: **for** each user $n \in \{1, 2, 3, \dots, N\}$ in parallel **do**
 - 5: Initialize divergence array $\text{DIV} = \{\}$
 - 6: **for** each image $j \in \left\{ X_{\mathcal{T}}^j \right\}_{j=1}^{\mathcal{B}_t}$ **do**
 - 7: $X_{\mathcal{T}}^j \leftarrow$ Augmentation
 - 8: Calculate BN statistics $\left\{ (\mu_{l_{c'}}^{\mathcal{T}_j}, (\sigma_{l_{c'}}^{\mathcal{T}_j})^2) \right\}$ of $X_{\mathcal{T}}^j$
 - 9: Calculate D using equation 1
 - 10: $\text{DIV} \leftarrow$ Store D
 - 11: **end for**
 - 12: $\tilde{\mathbf{X}}_t^n \leftarrow$ Select images with top- $K\%$ value in DIV
 - 13: perform pixel sampling on $\tilde{\mathbf{X}}_t^n$ with budget $b\%$ using equation 2,3,4,5
 - 14: update local model using equation 6
 - 15: **end for**
 - 16: update global model using equation 7
 - 17: copy updated global model to the local models
 - 18: **end for**
-

$$\mathcal{P}(x, y) = \sum_{c=1}^C \frac{|A_k^c(x, y)|}{|A_k(x, y)|} \log \frac{|A_k^c(x, y)|}{|A_k(x, y)|} \quad (3)$$

where $|A_k^c(x, y)|$ is the number of pixels of class c in the square region around pixel (x, y) .

The overall acquisition function for each image in $\tilde{\mathbf{X}}_t^n$ is given as,

$$\mathcal{U}_j(x, y) = \mathcal{H}_j(x, y) \odot \mathcal{P}_j(x, y) \quad (4)$$

and the corresponding pixels, sampled from the image for annotating are given as,

$$\mathcal{Q}^* = \{(x^*, y^*)\} \text{ where } (x^*, y^*) = \arg \max_{(x, y) \in R^2} \{\mathcal{U}_j(x, y)\}_{j=1}^{\tilde{\mathcal{B}}_t} \quad (5)$$

3.3. Adapting Local Models

After $b\%$ pixels have been selected from each image in $\tilde{\mathbf{X}}_t^n$, their corresponding labels are acquired from the local user. To adapt each of the local models f_θ^n to \mathcal{T} we update the parameters of their respective BN layers by minimizing the following cross-entropy loss on the annotated pixels,

$$\mathcal{L}_{CE} = -\frac{1}{|\mathcal{Q}^*|} \sum_{(x,y) \in \mathcal{Q}^*} \sum_{c=1}^C \mathbf{Y}(x,y,c) \log \mathbf{P}(i,j,c) \quad (6)$$

where, $\mathbf{Y}(x,y,c)$ is the label provided by the active learner at the (x,y) pixel of an image. It must be noted

3.4. Updating global model

Each of the N local models is updated after a test batch of images passes by each of them. The parameters of the local models are sent to the central server holding the global model, f_ϕ . Using the FedAvg method [23], the parameters, ϕ , of f_ϕ , are updated as shown below,

$$\phi(t) = \frac{1}{N} \sum_{n=1}^N \theta^n(t-1) \quad (7)$$

where $\theta^n(t-1)$ are the parameters of the f_θ^n after $(t-1)^{th}$ round of federated learning and $\phi(t)$ are the parameters of f_ϕ that will be deployed on the t^{th} round of federated learning. The updated f_ϕ is distributed back to the local users for their next round of incoming test images. The overall algorithm of **DrFRODA** is shown in Algo 1.

4. Experiments and Results

4.1. Dataset

- **CHAOS MRI:** CHAOS (Combined Healthy Abdominal Organ Segmentation) [12] includes Magnetic Resonance Imaging (MRI) of 20 subjects. MRI data sets are collected for two different sequences which are T1-DUAL and T2-SPIR. T1-DUAL also comprises two different types of signals: in-phase (IP) and out-of-phase (OOP). All the MRI datasets contain the annotations of four human internal organs: liver, left Kidney, right kidney and spleen.

- **DUKE MRI:**

The Duke liver dataset [22] contains the data of 105 patients. This dataset exhibits four distinct forms of contrasts, namely in phase, opposed phase, T1-weighted, and enhanced T1-weighted. In this dataset, only liver is annotated manually.

- **Prostate MRI:** A publicly available MRI dataset [20] has been used for prostate segmentation. It comprises manually annotated T2-weighted MRI from two different sites: Boston Medical Center (BMC) and Radboud University Medical Center (RUNMC). Each of the datasets comprises 30 MRI stacks.

4.2. Adaptations

- **CHAOS T2-SPIR to DUKE T2-SPIR** of CHAOS dataset is T2-weighted. DUKE dataset contains four different contrasts of MRI images. Hence, there is a domain

Table 1. DSC values for multi organ segmentation CHAOS T1-DUAL In Phase (IP) \rightarrow Out of Phase (OOP). The best results are highlighted in red and the second best results in blue. \dagger Results are shown on a held-out test split of the entire target domain testing data.

Comparison with existing TTA methods					
	Liver	L.Kid	R.Kid.	Spl.	mean
Source	87.77	37.97	18.92	67.31	52.99
TENT [34]	86.03	58.1	54.72	70.34	67.29
CoTTA [35]	86.38	52.8	58.27	71.06	67.13
DrFRODA (K = 50)	88.42	70.84	70.91	75.85	76.5
DrFRODA (K = 70)	88.53	70.86	71.93	76.06	76.84
Comparison with SOTA Offline ADA method. \dagger					
RIPU [36]	93.52	87.42	86.71	86.95	88.65
RIPU-SF [36]	93.54	85.69	84.29	86.69	87.55
DrFRODA (K = 50)	92.12	83.69	82.96	80.21	84.75
DrFRODA (K = 70)	92.11	83.25	83.16	80.94	84.87

shift between these two datasets. T2-SPIR of CHAOS data is considered the source domain, and DUKE dataset is considered as the target domain for liver segmentation.

- **CHAOS T1-DUAL IP to OOP** Although gradient echo sequences of IP and OOP of CHAOS T1-DUAL are collected with the same repetition time, the echo time values [26] are different causing the domain shift. IP and OOP are considered as source and target domains respectively.

- **BMC to RUNMC** BMC is used as the source, and RUNMC dataset as the target domain.

4.3. Baseline Methods and Metric

We compare DrFRODA with state-of-the-art (SOTA) TTA methods, TENT [34] and CoTTA [35]), as well as, with the SOTA offline UDA-AL/ADA method RIPU [36]. Two variations of RIPU are considered. The first with access to the source domain data, which is the standard implementation of RIPU and the second is w/o access to the source data or source-free RIPU, which we refer to as RIPU-SF. Since RIPU is an offline method, it needs a dedicated target domain training set, so we split the entirety of the target domain test set into training (80%) and testing (20%) split for RIPU. For a fair comparison, the performance of DrFRODA on this dedicated test split is compared with that of RIPU and RIPU-SF. Following standard practice in medical image segmentation [8], the Dice Score (DSC) is used as the performance metric.

4.4. Implementation Details

We use ResNet-18 backbone in Deeplabv3 [3]. We have used 1% pixel annotation from the active learner in each test batch. For updating the batch normalization layer we have used ADAM [15] optimizer with a learning rate 0.01.

Table 2. DSC values for single organ segmentation CHAOS T2SPIR \rightarrow DUKE (Liver segmentation) and BMC \rightarrow RUNMC (Prostate segmentation). The best results are highlighted in red and the second best results in blue. [†] Results are shown on a held-out test split of the entire target domain testing data.

	CHAOS \rightarrow DUKE	BMC \rightarrow RUNMC
Comparison with existing TTA methods.		
	Liver	Prostate
Source Only	12.77	74.47
TENT [34]	38.16	78.11
CoTTA [35]	38.54	77.06
DrFRODA(K = 50)	52.11	80.99
DrFRODA (K = 70)	52.30	81.10
Comparison with SOTA Offline ADA method. [†]		
RIPU [36]	78.81	89.06
RIPU-SF [36]	78.48	88.16
DrFRODA (K = 50)	63.92	84.68
DrFRODA (K = 70)	64.17	84.87

4.5. Results

Table 1 shows the results on CHAOS T1-DUAL IP \rightarrow OOP adaptation. Table 2 shows the results on CHAOS T2-SPIR \rightarrow DUKE and BMC \rightarrow RUNMC dataset adaptation for liver and prostate segmentation, respectively. In all those analyses we see that our approach outperforms the online TTA methods. For example, in Table 1 our method beats the best-performing online method by 9.71%. However, compared to offline method our approach shows some performance drop. For example, in Table 1 our methods shows 3.9% and 2.68% performance drop compared to RIPU and RIPU-SF. **Still it is a huge advantage because our method is totally online while RIPU is an offline method. Despite being an online method our method is showing competitive result with offline method.** The same pattern repeats in BMC \rightarrow RUNMC adaptation where we observe 4.19% and 3.29% performance drop compared to RIPU and RIPU-SF, respectively. However, in CHAOS T2-SPIR \rightarrow DUKE adaptation DrFRODA had much performance drop compared to RIPU. As mentioned earlier CHAOS comprises a combination of images with different contrasts. That is why DrFRODA could not capture all the distribution shifts in a single pass of every batch of images. RIPU was able to learn the distribution shift by training on same images with multiple passes. However, our method still shows 13.46% performance improvement compared to other TTA methods on this adaptation.

We also note that even without adaptation (source) in Table 1 the results on liver is quite satisfactory. Being the largest organ among all four classes, liver has the highest number of pixels. Hence with no adaptation, the prediction is a bit biased to segmenting liver. On the contrary, organs with less number of pixels such as left kidney, right kid-

Table 3. Comparison between Pixel and Area-based active annotation for CHAOS T1DUAL IP \rightarrow OOP adaptation under 1% annotation.

Organ	$K = 100$		$K = 50$	
	Pixel	Area	Pixel	Area
Liver	88.57	88.17	88.42	88.13
L. Kidney	71.34	67.86	70.84	66.92
R.Kidney	72.73	66.55	70.91	65.70
Spleen	76.7	76.59	75.85	76.81
mean	77.34	74.79	76.51	74.39

ney and spleen, result in comparatively less DSC. However, with the utilization of active learning, model performance in those classes improves significantly. A visual demonstration of performance using different methods is shown in Figure 3.

4.6. Ablation Studies

4.6.1 Comparison between Pixel vs Area Annotation

In the proposed method, the active learner annotated the pixels which are selected by the sampling function. However, in real life, annotating square regions is easier than annotating scattered pixels. In Table 3, we compare the performance of online adaptation using active learning through both pixel and area-based annotation under the same amount of budget. We consider $10\text{pixel} \times 10\text{pixel}$ square as a unit region for annotation. We follow the procedure described in [36] in order to perform area-based annotation by active learner. In Table 3 we observe that pixel-based annotation performs better than area-based annotation. Under the same budget, the pixel annotation only annotates the pixels where the model is least confident. However, in area annotation, the active learner has to annotate a region that includes both confident and less confident pixels for the network. Hence, we observe a drop of performance 2.55% and 1.12% for $K = 100$ and 50, respectively in area-based annotation.

4.6.2 Total Annotation fixed vs Total Annotation $\propto K$

In our work, we proposed an effective $K\%$ image selection technique from the current input batch. The active learner has a budget of $b\%$ pixels for each of the selected images. It means the total number of annotations is proportional to $K\%$ decreases. We do an ablation study where at first we select $K = 100$ (select all the images of the batch), then annotate $b\%$ of all images. This is the highest number of possible annotations. Now we decrease K , but keep the total number of annotations the same. It means with a decrease of K , the number of selected images decreases, but each image will get more than $b\%$ annotation. In Figure 4 we illustrate

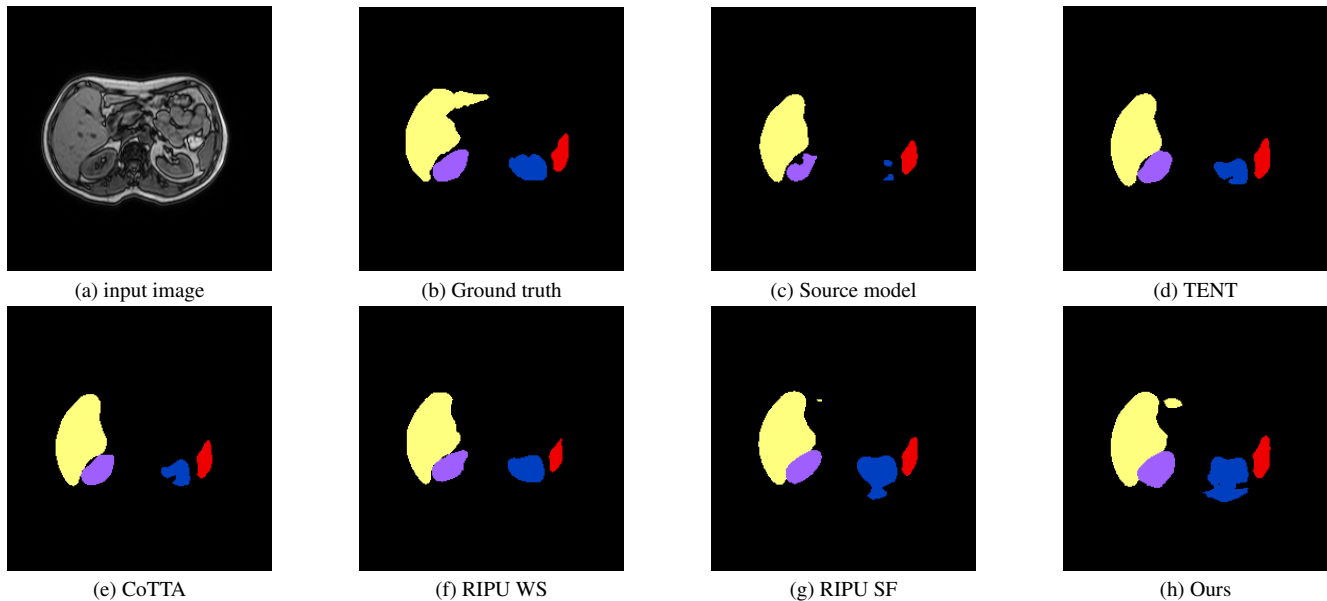


Figure 3. Segmentation results on CHAOS T1-DUAL for In Phase \rightarrow Out Phase adaptation. Liver, Left Kidney, Right Kidney and Spleen shown by yellow, purple, blue, and red colours, respectively.

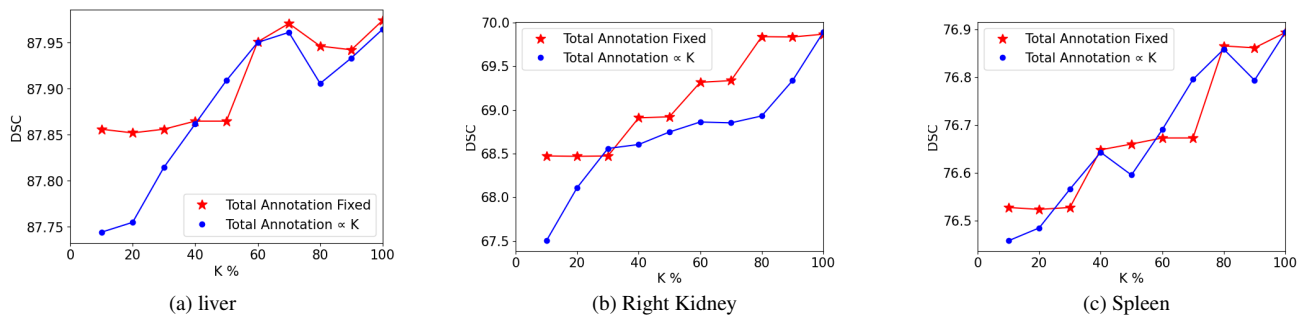


Figure 4. Performance comparison while keeping the total number of annotation fixed vs varying total number of annotation $\propto K$ (our original setting) for CHAOS T1-DUAL IP \rightarrow OOP adaptation.

how the segmentation performance of the network changes if the total number of annotations remains fixed vs a total number of annotations varies with K (our original setting). From the plots, we have two observations (i) in each case, if the value of K decreases which means less number of images are selected from the test batch, the DSC decreases. However the fall of DSC is not drastic. In the worst case, there is a drop of around 1% in DSC in right kidney segmentation when K is reduced from 100% by 50%. It means in exchange for a 1% performance loss, the active learner can concentrate on only 50% of the images of the batch which is really helpful for the active learner in an online application. (ii) If we compare the fixed number of pixel annotations and varying number of annotations with K , the performance of fixed number of annotation is slightly better than the other case. This is because the first case gets more annotation

than the other one. However the gap is not very much. It is because if we decrease K , less number of images are selected. Among those selected images, there is less amount of informative pixels which can enhance the performance of the model. As a result, even if the active learner provides more annotation, the performance of the network does not change much. More results and analysis will be added to supplementary documents.

5. Conclusion

In this paper, we present a novel distributed active learning-based online domain adaptive segmentation technique DrFRODA. We show the effectiveness of an innovative sampling strategy in active learning in facilitating online domain adaptation in a user-friendly manner. At the

same time, the confidentiality of personal information is maintained using a distributed system. Our method outperforms the existing TTA methods across datasets and shows performance close to offline methods in most of the datasets. Thus DrFRODA presents an effective solution in mitigating domain shifts in a collaborating manner for medical image segmentation while maintaining privacy, convenience and better performance than existing online methods.

References

- [1] PR Anisha, C Kishor Kumar Reddy, and LV Narasimha Prasad. A pragmatic approach for detecting liver cancer using image processing and data mining techniques. In *2015 International Conference on Signal Processing and Communication Engineering Systems*, pages 352–357. IEEE, 2015. [1](#)
- [2] Saeid Asgari Taghanaki, Kumar Abhishek, Joseph Paul Cohen, Julien Cohen-Adad, and Ghassan Hamarneh. Deep semantic segmentation of natural and medical images: a review. *Artificial Intelligence Review*, 54:137–178, 2021. [1](#)
- [3] L.-C. Chen, G. Papandreou, I. Kokkinos, K. Murphy, and A. L. Yuille. Deeplab: Semantic image segmentation with deep convolutional nets, atrous convolution, and fully connected CRFs. *IEEE Trans. Pattern Analysis and Machine Intelligence (TPAMI)*, 2017. [6](#)
- [4] Minghao Chen, Hongyang Xue, and Deng Cai. Domain adaptation for semantic segmentation with maximum squares loss. In *Proceedings of the IEEE/CVF International Conference on Computer Vision*, pages 2090–2099, 2019. [2](#)
- [5] Yarin Gal, Riashat Islam, and Zoubin Ghahramani. Deep Bayesian active learning with image data. In *Proceedings of the 34th International Conference on Machine Learning*, pages 1183–1192, 2017. [3](#)
- [6] Yufan He, Aaron Carass, Lianrui Zuo, Blake E Dewey, and Jerry L Prince. Autoencoder based self-supervised test-time adaptation for medical image analysis. *Medical image analysis*, 72:102136, 2021. [2](#)
- [7] John R Hershey and Peder A Olsen. Approximating the kullback leibler divergence between gaussian mixture models. In *2007 IEEE International Conference on Acoustics, Speech and Signal Processing-ICASSP'07*, volume 4, pages IV–317. IEEE, 2007. [5](#)
- [8] Minhao Hu, Tao Song, Yujun Gu, Xiangde Luo, Jieneng Chen, Yinan Chen, Ya Zhang, and Shaoting Zhang. Fully test-time adaptation for image segmentation. In *Medical Image Computing and Computer Assisted Intervention—MICCAI 2021: 24th International Conference, Strasbourg, France, September 27–October 1, 2021, Proceedings, Part III 24*, pages 251–260. Springer, 2021. [2](#), [6](#)
- [9] Nabil Ibtehaz and M Sohel Rahman. Multiresunet: Rethinking the u-net architecture for multimodal biomedical image segmentation. *Neural networks*, 121:74–87, 2020. [1](#)
- [10] Ajay J Joshi, Fatih Porikli, and Nikolaos Papanikolopoulos. Multi-class active learning for image classification. In *2009 IEEE conference on computer vision and pattern recognition*, pages 2372–2379. IEEE, 2009. [3](#)
- [11] Neerav Karani, Ertunc Erdil, Krishna Chaitanya, and Ender Konukoglu. Test-time adaptable neural networks for robust medical image segmentation. *Medical Image Analysis*, 68:101907, 2021. [2](#)
- [12] A Emre Kavur, N Sinem Gezer, Mustafa Barış, Sinem Aslan, Pierre-Henri Conze, Vladimir Groza, Duc Duy Pham, Soumick Chatterjee, Philipp Ernst, Savaş Özkan, et al. Chaos challenge-combined (ct-mr) healthy abdominal organ segmentation. *Medical Image Analysis*, 69:101950, 2021. [6](#)
- [13] Katherine K Kim, Jill G Joseph, and Lucila Ohno-Machado. Comparison of consumers’ views on electronic data sharing for healthcare and research. *Journal of the American Medical Informatics Association*, 22(4):821–830, 2015. [1](#), [2](#)
- [14] SangMook Kim, Sangmin Bae, Hwanjun Song, and Se-Young Yun. Re-thinking federated active learning based on inter-class diversity. In *Proceedings of the IEEE/CVF Conference on Computer Vision and Pattern Recognition*, pages 3944–3953, 2023. [3](#)
- [15] Diederik P Kingma and Jimmy Ba. Adam: A method for stochastic optimization. *arXiv preprint arXiv:1412.6980*, 2014. [6](#)
- [16] James Kirkpatrick, Razvan Pascanu, Neil Rabinowitz, Joel Veness, Guillaume Desjardins, Andrei A Rusu, Kieran Milan, John Quan, Tiago Ramalho, Agnieszka Grabska-Barwinska, et al. Overcoming catastrophic forgetting in neural networks. *Proceedings of the national academy of sciences*, 114(13):3521–3526, 2017. [3](#)
- [17] Ali Sami Kivrak, Yahya Paksoy, Cengiz Erol, Mustafa Koplay, Seda Özbek, and Fatih Kara. Comparison of apparent diffusion coefficient values among different mri platforms: a multicenter phantom study. *Diagn Interv Radiol*, 19(6):433–437, 2013. [2](#)
- [18] Shuang Li, Binhui Xie, Qiuxia Lin, Chi Harold Liu, Gao Huang, and Guoren Wang. Generalized domain conditioned adaptation network. *IEEE Transactions on Pattern Analysis and Machine Intelligence*, 44(8):4093–4109, 2021. [2](#)
- [19] Jonathan Feng-Shun Lin and Dana Kulić. Online segmentation of human motion for automated rehabilitation exercise analysis. *IEEE Transactions on Neural Systems and Rehabilitation Engineering*, 22(1):168–180, 2013. [1](#)
- [20] Quande Liu, Qi Dou, Lequan Yu, and Pheng Ann Heng. Ms-net: multi-site network for improving prostate segmentation with heterogeneous mri data. *IEEE transactions on medical imaging*, 39(9):2713–2724, 2020. [6](#)
- [21] Xiaowei Liu, Lei Yang, Jianguo Chen, Siyang Yu, and Keqin Li. Region-to-boundary deep learning model with multi-scale feature fusion for medical image segmentation. *Biomedical Signal Processing and Control*, 71:103165, 2022. [1](#)
- [22] Jacob A. Macdonald, Zhe Zhu, Brandon Konkel, Maciej Mazurowski, Walter Wiggins, and Mustafa Bashir. Duke liver dataset (mri), Mar. 2022. [6](#)
- [23] Brendan McMahan, Eider Moore, Daniel Ramage, Seth Hampson, and Blaise Aguerre y Arcas. Communication-efficient learning of deep networks from decentralized data. In *Artificial intelligence and statistics*, pages 1273–1282. PMLR, 2017. [3](#), [4](#), [6](#)

- [24] Jiayu Miao, Zongxin Yang, Leilei Fan, and Yi Yang. Fed-seg: Class-heterogeneous federated learning for semantic segmentation. In *Proceedings of the IEEE/CVF Conference on Computer Vision and Pattern Recognition*, pages 8042–8052, 2023. [3](#)
- [25] Shuaicheng Niu, Jiaxiang Wu, Yifan Zhang, Yaofu Chen, Shijian Zheng, Peilin Zhao, and Mingkui Tan. Efficient test-time model adaptation without forgetting. In *International conference on machine learning*, pages 16888–16905. PMLR, 2022. [3](#)
- [26] Miguel Ramalho, Vasco Herédia, Rafael OP de Campos, Brian M Dale, Rafael M Azevedo, and Richard C Semelka. In-phase and out-of-phase gradient-echo imaging in abdominal studies: intra-individual comparison of three different techniques. *Acta Radiologica*, 53(4):441–449, 2012. [6](#)
- [27] Marc A Rodwin. Patient data: property, privacy & the public interest. *American Journal of Law & Medicine*, 36(4):586–618, 2010. [1](#), [2](#)
- [28] Olaf Ronneberger, Philipp Fischer, and Thomas Brox. U-net: Convolutional networks for biomedical image segmentation. In *Medical Image Computing and Computer-Assisted Intervention–MICCAI 2015: 18th International Conference, Munich, Germany, October 5-9, 2015, Proceedings, Part III 18*, pages 234–241. Springer, 2015. [1](#)
- [29] Neeraj Sharma and Lalit M Aggarwal. Automated medical image segmentation techniques. *Journal of medical physics/Association of Medical Physicists of India*, 35(1):3, 2010. [1](#)
- [30] Yanyao Shen, Hyokun Yun, Zachary C. Lipton, Yakov Kro-nrod, and Animashree Anandkumar. Deep active learning for named entity recognition. In *International Conference on Learning Representations*, 2018. [3](#)
- [31] Inkyu Shin, Dong-Jin Kim, Jae Won Cho, Sanghyun Woo, Kwanyong Park, and In So Kweon. Labor: Labeling only if required for domain adaptive semantic segmentation. In *Proceedings of the IEEE/CVF International Conference on Computer Vision*, pages 8588–8598, 2021. [4](#)
- [32] Bernardo Camajori Tedeschini, Stefano Savazzi, Roman Stoklasa, Luca Barbieri, Ioannis Stathopoulos, Monica Nicoli, and Luigi Serio. Decentralized federated learning for healthcare networks: A case study on tumor segmentation. *IEEE Access*, 10:8693–8708, 2022. [1](#)
- [33] Yi-Hsuan Tsai, Wei-Chih Hung, Samuel Schuler, Kihyuk Sohn, Ming-Hsuan Yang, and Manmohan Chandraker. Learning to adapt structured output space for semantic segmentation. In *Proceedings of the IEEE conference on computer vision and pattern recognition*, pages 7472–7481, 2018. [2](#)
- [34] Dequan Wang, Evan Shelhamer, Shaoteng Liu, Bruno Olshausen, and Trevor Darrell. Tent: Fully test-time adaptation by entropy minimization. *arXiv preprint arXiv:2006.10726*, 2020. [1](#), [3](#), [4](#), [6](#), [7](#)
- [35] Qin Wang, Olga Fink, Luc Van Gool, and Dengxin Dai. Continual test-time domain adaptation. In *Proceedings of the IEEE/CVF Conference on Computer Vision and Pattern Recognition*, pages 7201–7211, 2022. [2](#), [3](#), [4](#), [6](#), [7](#)
- [36] Binhui Xie, Longhui Yuan, Shuang Li, Chi Harold Liu, and Xinjing Cheng. Towards fewer annotations: Active learning via region impurity and prediction uncertainty for domain adaptive semantic segmentation. In *Proceedings of the IEEE/CVF Conference on Computer Vision and Pattern Recognition*, pages 8068–8078, 2022. [1](#), [2](#), [3](#), [5](#), [6](#), [7](#)
- [37] Binhui Xie, Longhui Yuan, Shuang Li, Chi Harold Liu, Xinjing Cheng, and Guoren Wang. Active learning for domain adaptation: An energy-based approach. In *Proceedings of the AAAI Conference on Artificial Intelligence*, volume 36, pages 8708–8716, 2022. [4](#)
- [38] Chen Zhang, Yu Xie, Hang Bai, Bin Yu, Weihong Li, and Yuan Gao. A survey on federated learning. *Knowledge-Based Systems*, 216:106775, 2021. [1](#)